Towards an Optical Lattice Clock Based on Neutral Mercury

Michael Petersen, Daniel Magalhães, Cipriana Mandache, Ouali Acef,
André Clairon and Sébastien Bize
LNE-SYRTE
Observatoire de Paris
Paris, France 75014
Email: michael.petersen@obspm.fr
Telephone: +33 (0)1 40512222
Fax: +33 (0)1 43 25 55 42

***Abstract*— We are investigating the possibilities of using neutral mercury as a new species to realize a highly accurate atomic clock using the non-perturbing dipole lattice trapping scheme. Typically, accuracy below 10^{-17} is targeted. This proceeding outlines some properties of neutral mercury which are relevant to an optical lattice clock. We also present our on-going work towards the realization of the mercury optical lattice clock. Design considerations are made about the main subsystems. Recent work on these subsystems is described.**

I. Introduction

In the past few years, intense efforts have been devoted worldwide to the development of a new generation of atomic clocks based on optical transitions. These efforts have been reenforced by the advent of the optical frequency comb technology. For instance, optical clocks based on trapped $^{199}Hg^{+}$ and Al^{+} ions are now clearly surpassing atomic fountain clocks with accuracies below 10^{-16} [1]. Optical clocks using neutral atoms are reaching accuracies near or below 10^{-15} [2], [3]. These achievements have started impacting the applications of high accuracy atomic clocks. For example, recent absolute frequency measurements of the $^{199}Hg^{+}$ optical clock are leading to improved test of the stability of the fine structure constant α [4]. Several atomic transitions in the optical domain are now recognized by BIPM[1] as secondary representations of the SI second.

In this proceeding, we are introducing a project aiming to develop an optical lattice clock [5], [6] based on neutral mercury. Like for other optical lattice clocks, the goal is to combine the advantages of a trapped ion, where the clock transition is probed in the Lamb-Dicke regime, with those of neutral atoms, where a large ensemble of atoms can be sampled simultaneously. As shown below, several atomic properties of Hg are making it an interesting candidate for reaching ultimate accuracy. Also, introducing a new atom with a relatively high sensitivity to α variation [7] will increase the number of possibilities to perform fundamental physics tests. In the future, LNE-SYRTE will operate two microwave clocks (based on ^{87}Rb and ^{133}Cs hyperfine transitions [8], [9]) and two optical lattice clocks based on Sr and Hg.

[1]Bureau International des Poids et Mesures

TABLE I
The natural isotopes of mercury[11].

Isotope	Abundance (%)	Nuclear spin	Magnetic moment
196	0.15	0	0
198	10.1	0	0
199	17.0	1/2	+0.5059
200	23.1	0	0
201	13.2	3/2	-0.5602
202	29.6	0	0
204	6.85	0	0

In this proceeding, we also give some design considerations concerning some important subsystems and report on our on-going work to develop these subsystems.

II. Properties of mercury relevant to an optical lattice clock

A. Atomic properties and laser cooling

Mercury has an atomic number of 80 and an average atomic mass of 200.59 m_u. It has 7 natural isotopes, 2 fermions and 5 bosons (see table I). At least 6 of them have a natural occurrence higher than 5% and are therefore practically usable for a clock. ^{196}Hg with a 0.15% natural occurrence is less favorable.

Compared to other atoms considered so far for optical lattice clocks, Hg has a much higher vapor pressure. The vapor pressure at 300 K is 0.3 Pa. A vapor pressure between 10^{-5} and 10^{-4} Pa, well suited for a vapor cell magneto-optic trap, is met near -55 ± 5 °C, a temperature which is easily reached in vacuum with Peltier thermoelectric coolers. Avoiding an oven at very high temperature ($\sim$ 600 °C for Sr typically) is favorable for better controlling the blackbody radiation shift. Pumping of mercury can be done for instance with a cold surface. The vapor pressure goes down to 10^{-7} Pa near -80 °C [10].

Like strontium or ytterbium, mercury has an alkaline-earth-like electronic structure shown in fig. 1. The ground 6 $^1S_0$

1-4244-0647-1/07/$20.00 ©2007 IEEE

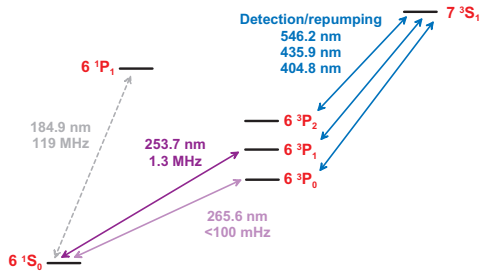

Fig. 1. The lowest energy levels of mercury.

state is a singlet state with no spin for the bosonic isotope and a purely nuclear spin of 1/2 and 3/2 for the fermionic isotopes ^{199}Hg and ^{201}Hg (see table I). The strongly allowed transition to 6 ^{1}P$_1$ has a wavelength of 185 nm and is not well suited for laser cooling because this wavelength is very difficult to synthesize and because the short lifetime of the 6 ^{1}P$_1$ state of 1.3 ns corresponds to quite a high Doppler temperature of 2.8 mK. Instead, the intercombination transition to the 6 ^{3}P$_1$ has a wavelength of 254 nm which is less challenging to synthesize. Also, the natural linewidth of 1.3 MHz corresponds to a favorable Doppler temperature of 31 μK while being strong enough for magneto-optic trapping. The saturation intensity of this transition is 10 mW cm^{-2}.

B. Properties of the clock transition

The clock transition is the intercombination $^1S_0 \rightarrow {}^3P_0$ transition at 265.6 nm. In the fine-structure approximation, this $J = 0 \rightarrow J = 0$ transition is electric-dipole forbidden at all orders. In the fermionic isotopes ^{199}Hg and ^{201}Hg with non-zero nuclear spin, the transition becomes weakly allowed by hyperfine mixing as in ^{87}Sr, ^{171}Yb and ^{173}Yb. The mixing coefficients and the lifetime of the metastable $^3P_0$ state were both calculated and measured in 1967 [12]. The corresponding linewidths are close to 100 mHz for both fermionic isotopes. For these isotopes, the clock states have small degeneracy (total spin of 1/2 and 3/2) which is favorable compared to ^{87}Sr which has a total spin of 9/2 in the ground state. Bosonic isotopes are good candidates to apply the scheme of [13] where a static magnetic field is used to quench the $^3P_0$ state to allow the excitation of the clock transition.

C. Blackbody radiation shift

Blackbody radiation shift is a significant shift for all atomic frequency standards both in the microwave and the optical domains. For instance, it is one of the largest shifts in atomic fountain clocks (-1.7×10^{-14} at 300 K) and requires difficult measurements to be controlled to better than the percent level [14]. It is the largest shift in optical lattice clock based on ^{87}Sr (-5.5×10^{-15} at 300 K [15]). In the future, the blackbody radiation shift could be the limiting factor to the accuracy of several optical clocks at the level of a few parts in 10^{17}. One of the interesting features of Hg is its blackbody radiation shift smaller than for other atoms considered for optical lattice clocks. The shift is estimated to be -2.4×10^{-16} at 300 K [16], 10 times smaller than for Yb and 20 times smaller than for Sr. Blackbody radiation shift at 300 K in Hg$^+$ and In$^+$ is significantly smaller (factor of ~ 3). It is much smaller in Al$^+$ (factor of 30)[17].

TABLE II
BLACKBODY RADIATION SHIFT AT 300 K FOR SOME NEUTRAL ATOM CLOCKS.

Atom	transition	fractional shift due to blackbody radiation at 300 K
Cs	$F = 3 \longrightarrow F = 4$	$-1.7 \cdot 10^{-14}$
Rb	$F = 1 \longrightarrow F = 2$	$-1.3 \cdot 10^{-14}$
Sr	^{1}S$_0 \longrightarrow {}^3$ P$_0$	$-5.5 \cdot 10^{-15}$
Ca	^{1}S$_0 \longrightarrow {}^3$ P$_1$	$-2.2 \cdot 10^{-15}$
Yb	^{1}S$_0 \longrightarrow {}^3$ P$_0$	$-2.4 \cdot 10^{-15}$
Mg	^{1}S$_0 \longrightarrow {}^3$ P$_0$	$-3.9 \cdot 10^{-16}$
Hg	^{1}S$_0 \longrightarrow {}^3$ P$_0$	$-2.4 \cdot 10^{-16}$

D. Magic wavelength and dipole lattice trapping

Feasibility of the optical lattice clock scheme relies on the existence of a so-called magic wavelength, where the ac-polarizabilities of both clock states are equal. For mercury, such magic wavelength exists between the two strongly allowed transitions from 6 ^{3}P$_0$ to 7 ^{3}S$_1$ at 405 nm and from 6 ^{3}P$_0$ to 6 ^{3}D$_1$ at 297 nm [16]. A first calculation gave a magic wavelength of 342 nm [18]. A more recent calculation gives 360 nm [19]. The recoil frequency corresponding to this wavelength is 7.7 kHz. To achieve a trap depth of 1 recoil, the required intensity is 5.1 kW cm^{-2} for a traveling wave.

E. Sensitivity to α variation

As mentioned above, comparing highly accurate atomic clocks based on different atomic species leads to tests of the stability of fundamental constants. The sensitivity of the ^{1}S$_0 \rightarrow {}^3$P$_0$ transition in mercury to variation of fundamental constants has been evaluated in [7]. As for all optical transitions, it is mostly sensitive to variation of the fine-structure constant α with the following sensitivity: $d\ln(\omega_{at}) = 0.81\, d\ln(\alpha)$. This sensitivity is high compared to other atoms used in optical lattice clocks.

III. TOWARDS COOLING AND TRAPPING OF MERCURY

Magneto-optical trapping (MOT) of neutral mercury is a prerequisite for the realization of an atomic clock. It is also an attractive goal to laser cool a new atomic species which often gives access to better knowledge of atomic properties. This is particularly true for mercury with at least 6 practically usable isotopes.

A. MOT chamber

In our proposed design, the MOT will be loaded by a 2 dimensional magneto-optical trap (2D-MOT) [20]. The high vapor pressure of mercury makes it possible to load this 2D-MOT from a background vapor while keeping the vacuum

chamber at room temperature as it is done for Cs or Rb. The Hg background pressure will be held at an appropriate level for the 2D-MOT (10^{-5} and 10^{-4} Pa) using the Hg source described in the next subsection. A 1.5 mm diameter and 10 mm long hole will let atoms effusing horizontally from the 2D-MOT towards the center of the MOT, while strongly reducing the conductance for the background gas. The MOT center is 7 cm away from the output of the 2D-MOT. Having in mind the clock application, the vacuum chamber parts are made of non-magnetic material (TA6V titanium alloy). The windows are made with AR-coated UV grade fused silica which transmits the cooling and clock wavelengths. Water cooled MOT coils are designed to create a magnetic field gradient of $\sim$ 75 G cm^{-1} for a current of 10 A and a power dissipation of $\sim$ 50 W. Values are similar for the 2D-MOT coils with a dissipated power of $\sim$ 150 W. According to some preliminary numerical calculations, the optimum gradient is about $\sim$ 60 G cm^{-1}, a quite high value due to the heavy atomic mass. In the present form, the vacuum chamber includes a time of flight zone which should help optimizing and studying cooling and trapping.

B. Mercury source

Since mercury has an exceptionally high vapor pressure of 0.3 Pa at room temperature, the source of mercury for the 2D-MOT is cooled down to reduce and control the mercury pressure.

Liquid mercury is placed in a small copper bowl glued to the cold surface of a two-stage Peltier thermoelectric cooler placed inside the vacuum. The hot side of the thermoelectric cooler is attached to a water-cooled block of copper whose temperature is maintained near 10 °C. The Peltier element can sustain a temperature difference of 81 °C which is more than enough to bring the mercury temperature to the required -55 ± 5 °C. In addition to the mercury source, the 2D-MOT chamber includes a getter pump to pump other residual gases. So far experiments show that we can release and recapture mercury by controlling the power to the Peltier element although the recapture process is slower and not completely perfect. This is probably due to mercury being captured in the walls of the vacuum chamber. No particular care has been taken to purify mercury. However, the noticeable release of nitrogen and hydrogen by the mercury source remains at least one order of magnitude smaller than the released mercury and should not be detrimental to the 2D-MOT. Additionally, the getter pump seems to tolerate exposure to mercury vapor. Notice that pumping of mercury in the MOT chamber is achieved by a device similar to the mercury source. A copper surface is maintained below -100 °C by means of a 6-stage Peltier thermoelectric cooler placed inside the vacuum. This pump is complemented by an ion pump and a getter pump.

C. Cooling light source

One of the challenging tasks in this project is to synthesize the 254 nm light for lasercooling and atomic detection on the $^1S_0 \rightarrow {}^3P_1$ transition. Typically, several 100 mW of power are required. Additionally, in order to reach the lowest temperature, the laser linewidth and frequency fluctuations must be a small fraction of the natural linewidth of 1.3 MHz at 254 nm which is significantly more constraining than for instance Rb (6 MHz natural linewidth at 780 nm).

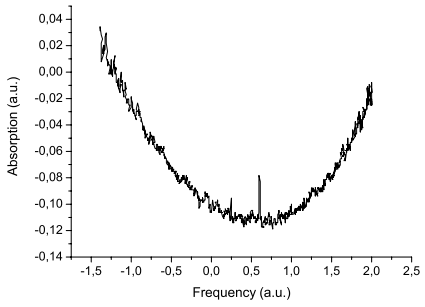

Fig. 2. Measured saturated absorbtion spectrum of ^{200}Hg at 254 nm. The measurement is performed on room temperature quartz cell with an interaction length of 1 mm.

The laser source is based on a near infrared diode-pumped Yb:YAG thin-disk laser. This laser delivers 7 W of CW single frequency laser light at 1015 nm. This light is frequency doubled in a commercial cavity-enhanced second harmonic generation (SHG) unit using a 90° phase matched LBO crystal at $\sim$ 216 °C. Up to 3 W have been obtained at 508 nm. The second SHG is performed with a home made system inspired by the work of [21]. An AR-coated 7 mm long β-barium borate (BBO) crystal is used, for which type I angle-tuned phase matching is achieved at $\theta = 51.2°$. The ring cavity is made of one flat 98.5 % reflecting input coupler, of one flat mirror and two curved mirrors with 50 mm radius of curvature. The round trip length is 241 mm and the size of the waist in the crystal is $\sim$ 28 μm. Light at 254 nm is extracted through one of the curved mirrors which is coated for maximum transmission at this wavelength and made of UV grade fused silica. More than 600 mW of continuous light at 254 nm has been obtained from this system.

The next step to make this source suitable for lasercooling is to stabilize the laser to the atomic line. In order to do so, we perform saturated absorbtion spectroscopy. Thanks to the high vapor pressure of mercury, a room temperature cell with an interaction length of 1 mm is well suited for the task. Cells have been realized by condensing a small quantity of purified mercury in a commercially available quartz cell. For probing the cell, a small fraction of light reflecting off the output coupler and transmitted through the input coupler (also made of UV grade fused silica) was used. A Doppler free spectrum was observed for the six abundant isotopes, as exemplified in figure 2 with the ^{200}Hg spectrum line. The Doppler linewidth is close to 1 GHz FWHM. Using a 5 mm cell, the Doppler spectrum of the 0.15% abundant ^{196}Hg isotope was also observed.

At this point, the next step would have been to stabilize the laser light to the saturated absorption peak by acting on the

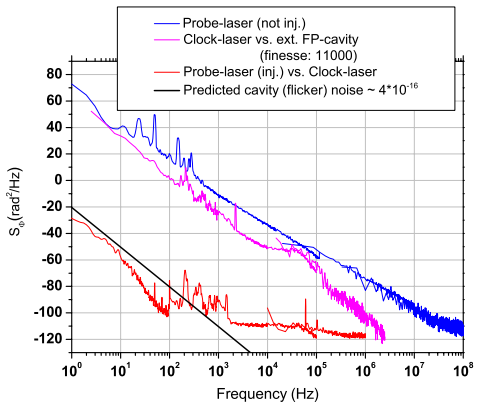

Fig. 3. Phase noise power spectral density of the Yb-doped fiber laser and of the semiconductor DFB laser used as the clock laser at 1062.5 nm. Phase noise is measured at the optical carrier frequency of 2.8×10^{14} Hz. The graph also shows the phase noise between the fiber laser and the semiconductor laser injection-locked with the fiber laser. The solid black indicates the phase noise PSD equivalent to the predicted thermal noise limit of the cavity (flicker frequency noise behavior at the level of 3 parts in 10^{16}).

PZT driven output coupler of the thin-disk laser. Unfortunately, a failure of this laser stopped us from completing this step. The laser has been under repair for several months. The previously described steps already demonstrate the feasibility of a laser source suitable for cooling mercury. This work will be pursued when the laser returns. Similar work has been done simultaneously, as reported in [22].

IV. Development of an ultra stable laser source at 265.6 nm

Exciting the clock $^1S_0 \rightarrow {}^3P_0$ transition requires an ultra stable laser source at 265.6 nm. About 10 mW of power is required to reach a Rabi frequency of several kHz over the entire size of the MOT. This excitation rate should be sufficient for preliminary investigations of the clock transition on atoms free-falling from the MOT as done in [23], [24]. In the long run, performing high resolution spectroscopy in the dipole lattice trap and running the clock requires much less power.

To synthesize this wavelength, a narrow-line Yb-doped fiber laser is used at 1062.5 nm (4 times the required wavelength). Such laser has intrinsically low frequency noise and therefore constitutes a convenient starting point for an ultra stable light source. The light from this laser will be stabilized to a reference Fabry-Pérot cavity and sent to an optical frequency comb for frequency measurements and comparisons with other clocks. As a second step, the stabilized light is amplified and frequency doubled twice.

A. Clock laser at 1062.5 nm

The 1062.5 nm Yb-doped fiber laser is a commercially available laser [25]. Due to the small tunability of these lasers, the laser must be customized to meet the required wavelength. The wavelength can be temperature-controlled (slow tuning) in a $\sim$ 650 pm range around 1062.467 nm. Fast (several 10 kHz bandwidth), small amplitude tuning is achieved with a PZT.

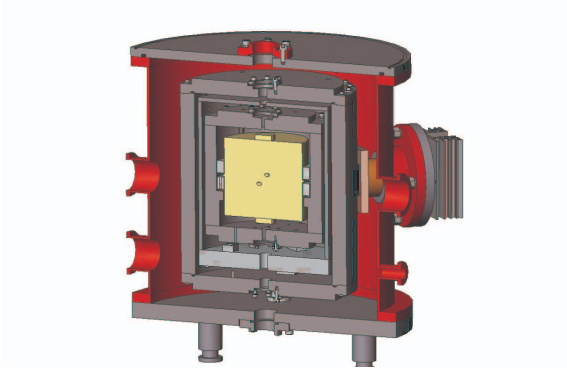

Fig. 4. A sectioned view of the ultra-stable cavity assembly.

Thanks to an output amplifier stage, the laser has an adjustable output power up to 200 mW (PM fiber coupled). As a first step, we have carefully characterized the noise properties of the free-running fiber laser. Both the relative intensity noise (RIN) and the frequency noise have been measured at several output powers. The RIN is typically less than -100 dB.Hz^{-1} at Fourier frequencies higher than 1 Hz, less than -135 dB.Hz^{-1} at Fourier frequencies higher than 100 kHz and less than -160 dB.Hz^{-1} at Fourier frequencies higher than 1 MHz. The frequency noise has been measured against a Fabry-Pérot cavity (cavity in vacuum, with INVAR spacer, 10000 finesse). The frequency of the light from the laser is frequency shifted with a 150 MHz acousto-optic modulator (AOM) and sent to the cavity, whose resonance is detected using the Pound-Drever-Hall method [26]. A fast voltage controlled oscillator (VCO) driving the AOM is used to lock to the cavity with a bandwidth greater than 1 MHz. Within the locking bandwidth, the frequency of the RF signal delivered by the VCO reflects frequency fluctuations between the laser and the analyzing cavity. This signal is analyzed with a frequency-to-voltage converter or a RF spectrum analyzer. Figure 3 shows the laser noise power spectral density (PSD) deduced from these measurements. The linewidth deduced from this measurement, based on the integral of the phase noise PSD, is 3 kHz.

B. Reference cavity

The clock laser will be stabilized to an ultra stable Fabry-Pérot reference cavity. The design of this system is inspired by previous work reported for instance in [27], [28], [29], [30]. A cavity with a vertical configuration will be used. Finite element calculation have been used to reduce the sensitivity to acceleration to the 10^{-11} m s^{-2} range. The ULE glass spacer has a length of 100 mm. Fused silica mirrors with a design finesse of 300000 will be used. We predict that this configuration should lead to a thermal noise limit of $\sim 3\times10^{-16}$ for the fractional frequency instability [31]. Note however that fused silica mirrors on an ULE spacer lead to an increased temperature sensitivity. Stability in the low 10^{-16} range with fused silica mirrors has not yet been demonstrated.

The cavity will be placed inside a double layer vacuum enclosure designed to allow operation well below room tem-

perature, where the temperature sensitivity of the cavity assembly, including the fused silica mirrors goes to zero. Inside the temperature stabilized enclosure, 2 aluminium layers are added to further increase passive shielding of temperature fluctuations. This setup is schematized in figure 4. This assembly will be placed on a commercial passive isolation platform surrounded by a custom made acoustic enclosure. Given the residual accelerations measured on the isolation platform (with a seismometer), an acceleration sensitivity less than 10^{-10} m s^{-2} is enough to bring the corresponding frequency noise below the thermal noise limit. This system will be tested by comparing it to a second similar system currently under development in our lab for other applications.

C. 265.6 nm frequency generation

The first step to generate the 265.6 nm radiation is to amplify the ultra stable light at 1062.5 nm. This is done using a DFB (distributed feedback) semiconductor laser delivering up to 500 mW at this wavelength (250 mW practically usable after the necessary optical isolators, due to a poor mode quality). This laser is stabilized to the ultra stable light source either by a phase-lock loop (for tunability during preliminary work) or by injection-locking (for clock operation with low noise). The phase noise between the injection-locked DFB laser and the seed fiber laser has been tested (see figure 3). Noise in this measurement is limited by the measurement system (electronic noise, uncompensated free space propagation of laser beams,etc). The noise added in the injection-locking process is negligible for our application.

The output of the DFB laser diode is frequency doubled twice. First doubling is realized with a 20 mm long PP-KTP crystal. The build-up cavity has a 8% input coupler and a waist in the crystal of ~ 36 μm. The measured overall conversion efficiency is 64 % which leads to 160 mW at 531 nm. The second doubling cavity is similar to the one described in section III. 5 mW of 265.6 nm radiation are generated, conversion efficiency being currently limited by the loss in one of the build-up cavity mirrors. Note, however that this power should be sufficient for the preliminary investigation of the clock transition. Both cavities are currently locked by modulating the cavity length at 31.5 kHz through a PZT driven mirror also used to apply the feedback loop corrections. This method implies that a small phase modulation is imprinted into the clock laser beam. Although this will not be a problem on the short term, high performance clock operation might require the use of a different locking scheme (such as the Hänsch-Couillaud scheme [32]) to remove this modulation. Figure 5 shows the measured RIN of the 265.6 nm light. The observed noise level will not be a limiting factor even for future clock operation at very high stability.

V. Conclusions

We have presented some features of neutral mercury that are making it an interesting candidate for a new optical lattice clock. We have reported on our on going effort to develop such an atomic clock. Sufficient laser power at the laser cooling wavelength of 254 nm has been obtained. Saturated absorption spectroscopy has also been observed and will be used to stabilize the laser source as required for laser cooling. A failure of the commercial laser is currently preventing us from completing this step. The vacuum system is now close to completion after the proposed solutions for controlling the mercury vapor pressure have been tested. Generation of 265.6 nm light for the clock transition by frequency quadrupling a 1062.5 nm source has been implemented with the appropriate power level. The development of an ultra stable reference at 1062.5 nm is under way.

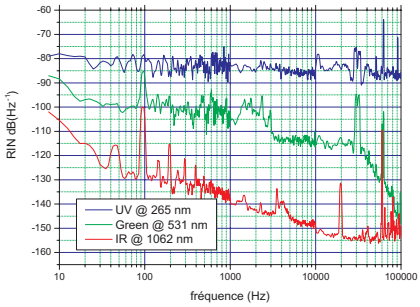

Fig. 5. The relative intensity noise (RIN) of the injection-locked DFB laser and of the frequency doubled 531 nm and frequency quadrupled 265.6 nm radiations.

Acknowledgment

The authors would like to acknowledge support from SYRTE technical services. SYRTE is Unité Mixte de Recherche du CNRS (UMR CNRS 8630). SYRTE is associated to Université Pierre et Marie Curie. This work is partly funded by the cold atom network IFRAF. This work received partial support from CNES.

References

[1] W. H. Oskay, S. A. Diddams, E. A. Donley, T. M. Fortier, T. P. Heavner, L. Hollberg, W. M. Itano, S. R. Jefferts, M. J. Delaney, K. Kim, F. Levi, T. E. Parker, and J. C. Bergquist, "Single-atom optical clock with high accuracy," *Physical Review Letters*, vol. 97, no. 2, p. 020801, 2006. [Online]. Available: http://link.aps.org/abstract/PRL/v97/e020801

[2] M. M. Boyd, A. D. Ludlow, S. Blatt, S. M. Foreman, T. Ido, T. Zelevinsky, and J. Ye, "[sup 87]sr lattice clock with inaccuracy below 10[sup -15]," *Physical Review Letters*, vol. 98, no. 8, p. 083002, 2007. [Online]. Available: http://link.aps.org/abstract/PRL/v98/e083002

[3] P. Lemonde et al., "An optical lattice clock with spin-polarized ^{87}Sr atoms," in *Proceedings of the 2007 EFTF-FCS conference*, 2007.

[4] T. M. Fortier, N. Ashby, J. C. Bergquist, M. J. Delaney, S. A. Diddams, T. P. Heavner, L. Hollberg, W. M. Itano, S. R. Jefferts, K. Kim, F. Levi, L. Lorini, W. H. Oskay, T. E. Parker, J. Shirley, and J. E. Stalnaker, "Precision atomic spectroscopy for improved limits on variation of the fine structure constant and local position invariance," *Physical Review Letters*, vol. 98, no. 7, p. 070801, 2007. [Online]. Available: http://link.aps.org/abstract/PRL/v98/e070801

[5] H. Katori, M. Takamoto, V. Pal'chikov, and V. Ovsiannikov, "Ultrastable optical clock with neutral atoms in an engineered ligth shift trap," *ArXiv:physics/0309043*, 2003.

[6] M. Takamoto and H. Katori, "Spectroscopy of the s[sub 0] - p[sub 0] clock transition of sr in an optical lattice," *Physical Review Letters*, vol. 91, no. 22, p. 223001, 2003. [Online]. Available: http://link.aps.org/abstract/PRL/v91/e223001

[7] E. J. Angstmann, V. A. Dzuba, and V. V. Flambaum, "Relativistic effects in two valence-electron atoms and ions and the search for variation of the fine-structure constant," *Physical Review A (Atomic, Molecular, and Optical Physics)*, vol. 70, no. 1, p. 014102, 2004. [Online]. Available: http://link.aps.org/abstract/PRA/v70/e014102

[8] Chapelet et al., "Comparisons between 3 fountain clocks at LNE-SYRTE," in *Proceedings of the 2007 EFTF-FCS conference*, 2007.

[9] S. Bize, P. Laurent, M. Abgrall, H. Marion, I. Maksimovic, L. Cacciapuoti, J. Grünert, C. Vian, F. Pereira dos Santos, P. Rosenbusch, P. Lemonde, G. Santarelli, P. Wolf, A. Clairon, A. Luiten, M. Tobar, and C. Salomon, "Advances in ^{133}Cs fountains," *C. R. Physique*, vol. 5, p. 829, 2004.

[10] F. E. Poindexter, "Mercury vapor pressure at low temperatures," *Physical Review*, vol. 26, no. 6, pp. 859–868, 1925. [Online]. Available: http://link.aip.org/link/?PR/26/859/1

[11] http://physics.nist.gov/PhysRefData/Handbook/Tables/mercurytable1.htm.

[12] M. Bigeon, "Probabilité de transition de la raie 6 1S0-6 3P0 du mercure," *Journal de Physique*, vol. 28, p. 51, 1967.

[13] A. V. Taichenachev, V. I. Yudin, C. W. Oates, C. W. Hoyt, Z. W. Barber, and L. Hollberg, "Magnetic field-induced spectroscopy of forbidden optical transitions with application to lattice-based optical atomic clocks," *Physical Review Letters*, vol. 96, no. 8, p. 083001, 2006. [Online]. Available: http://link.aps.org/abstract/PRL/v96/e083001

[14] P. et al., "Black body radiation shift in primary frequency standards," in *Proceedings of the 2007 EFTF-FCS conference*, 2007.

[15] S. G. Porsev and A. Derevianko, "Multipolar theory of blackbody radiation shift of atomic energy levels and its implications for optical lattice clocks," *Physical Review A (Atomic, Molecular, and Optical Physics)*, vol. 74, no. 2, p. 020502, 2006. [Online]. Available: http://link.aps.org/abstract/PRA/v74/e020502

[16] V. Pal'chikov, private communication (2004).

[17] T. Rosenband, W. M. Itano, P. O. Schmidt, D. B. Hume, J. C. J. Koelemeij, J. C. Bergquist, and D. J. Wineland, "Blackbody radiation shift of the 27al+ 1s0 - 3p0 transition," *arXiv:physics/0611125v2*, 2006.

[18] V. D. Ovsiannikov, V. G. Pal'chikov, H. Katori, and M. Takamoto, "Polarisation and dispersion of light shifts in highly stable optical frequency standards," *Quantum Electronics*, vol. 36, p. 3, 2006.

[19] V. Pal'chikov et al., "Optical lattice polarization effects on hyperpolarizability of alkaline-earth atoms," in *Proceedings of the 2007 EFTF-FCS conference*, 2007.

[20] K. Dieckmann, R. J. C. Spreeuw, M. Weidemüller, and J. T. M. Walraven, "Two-dimensional magneto-optical trap as a source of slow atoms," *Phys. Rev. A*, vol. 58, no. 5, pp. 3891–3895, Nov 1998.

[21] D. Berkeland, F. Cruz, and J. Bergquist, "Sum-frequency generation of continuous-wave light at 194 nm," *Applied Optics*, vol. 36, p. 4159, 1997.

[22] M. Scheid, F. Markert, J. Walz, J. Wang, M. Kirchner, and T. W. Hänsch, "750 mw continuous-wave solid-state deep ultraviolet laser source at the 253.7 nm transition in mercury," *Optics Letters*, vol. 32, no. 8, pp. 955–957, Apr. 2007.

[23] I. Courtillot, A. Quessada, R. Kovacich, A. Brusch, D. Kolker, J.-J. Zondy, G. Rovera, and P. Lemonde, "Clock transition for a future optical frequency standard with trapped atoms," *Phys. Rev. A*, vol. 68, p. 030501, 2003.

[24] C. W. Hoyt, Z. W. Barber, C. W. Oates, T. M. Fortier, S. A. Diddams, and L. Hollberg, "Observation and absolute frequency measurements of the [sup 1]s[sub 0]-[sup 3]p[sub 0] optical clock transition in neutral ytterbium," *Physical Review Letters*, vol. 95, no. 8, p. 083003, 2005. [Online]. Available: http://link.aps.org/abstract/PRL/v95/e083003

[25] The Yb-doped fiber laser is from Koheras.

[26] R. Drever, J. Hall, F. Kowalski, J. Hough, G. Ford, A. Munley, and H. Ward, "Laser phase and frequency stabilization using an optical resonator," *Appl. Phys B.*, vol. 31, p. 97, 1983.

[27] B. Young, F. Cruz, W. Itano, and J. Bergquist, "Visible lasers with subhertz linewidths," *Phys. Rev. Lett.*, vol. 82, p. 3799, 1999.

[28] S. A. Webster, M. Oxborrow, and P. Gill, "Vibration insensitive optical cavity," *Physical Review A (Atomic, Molecular, and Optical Physics)*, vol. 75, no. 1, p. 011801, 2007. [Online]. Available: http://link.aps.org/abstract/PRA/v75/e011801

[29] C. T. Taylor, M. Notcutt, and D. G. Blair, "Cryogenic, all-sapphire, fabry–perot optical frequency reference," *Review of Scientific Instruments*, vol. 66, no. 2, pp. 955–960, 1995. [Online]. Available: http://link.aip.org/link/?RSI/66/955/1

[30] L. Chen, J. L. Hall, J. Ye, T. Yang, E. Zang, and T. Li, "Vibration-induced elastic deformation of fabry-perot cavities," *Physical Review A (Atomic, Molecular, and Optical Physics)*, vol. 74, no. 5, p. 053801, 2006. [Online]. Available: http://link.aps.org/abstract/PRA/v74/e053801

[31] K. Numata, A. Kemery, and J. Camp, "Thermal-noise limit in the frequency stabilization of lasers with rigid cavities," *Physical Review Letters*, vol. 93, no. 25, p. 250602, 2004. [Online]. Available: http://link.aps.org/abstract/PRL/v93/e250602

[32] T. Hänsch and B. Couillaud, "Laser frequency stabilization by polarization spectroscopy of a reflecting reference cavity," *Opt. Commun.*, vol. 35, p. 441, 1980.